

## CRYSTAL STRUCTURE OF BARYLITE, $\text{BaBe}_2\text{Si}_2\text{O}_7$ (Use of Difference $F^2$ -Syntheses to Solve for Light Atoms in the Presence of Comparatively Heavy Ones)

K. K. Abrashev, V. V. Ilyukhin, and N. V. Belov

Institute of Crystallography, Academy of Sciences of the USSR

Translated from *Kristallografiya*, Vol. 9, No. 6,

pp. 816-827, November-December, 1964

Original article submitted July 20, 1964

The structural arrangement found in barylite is based on a  $[\text{Be}_2\text{O}_6]_\infty$  chain of the same type as that found in a number of recently analyzed Be silicates (e.g., bertrandite and euclase) and also in isostructural Zn silicates and phosphates. Barylite also shows another of the features previously noted for these structures, i.e., metaberylate chains encrusted with  $\text{SiO}_4$  orthotetrahedra. The chains are individual ones, but the attached  $\text{SiO}_4$  groups pair off with similar groups on neighboring chains to form  $\text{Si}_2\text{O}_7$  diorthogroups. Barylite shows quite marked hexagonal close-packing of the O anions, among which (in the ratio 1:7) the large Ba cations are to be found on equal terms with the oxygen ions. This makes the barylite structure the key to the apparently paradoxical, but quite usual, replacement of Be in Be minerals by appreciable proportions of Ba. Besides the main barylite structure analysis, an examination is made of a number of examples of the exposure of a light atom (Be) or Fourier patterns in the presence of heavy atoms, and the marked superiority of difference Patterson syntheses in this connection is noted.

The original material used in the investigation were some fine intergrowths of crystal kindly placed at our disposal by Professor K. Frondel (Harvard University), but subsequently some barylite crystals were received from A. G. Zhabin, who shares with Yu. P. Dikov the honor of the first discovery of barylite in the USSR (in the Vishnevye Hills) [1].

Barylite was discovered by Blomstrand in 1876, but his description was not completely accurate, for in his analysis Be was taken as Al. A second discovery allowed Aminoff [2] to establish that the chemical formula of the mineral was  $\text{BaBe}_2\text{Si}_2\text{O}_7$ , and to refer it (from its optical properties) to the rhombic holohedral class mmm, observing in the original arrangement the "instinctive" tendency of classical mineralogy, the choice of the a axis normal to the close-packing planes.

In 1942 Ygberg [3] reported the unit cell parameters for an orthorhombic lattice:  $a = 9.79$ ,  $b = 11.65$ ,  $c = 4.63$  Å (interchanging a and c axes). The unit cell contained  $Z = 4$  formula units of

$\text{BaBe}_2\text{Si}_2\text{O}_7$ . The possible space groups were given as Pmma and Pnma. The author considered the latter to be more probable. The same results were obtained by Smith in 1956 [4]. In Strunz's tables [5], barylite is given as an island ("clustered") sorosilicate.

In the first stage of the x-ray structural analysis we were hindered by the lack of single crystals, due to the characteristic and uniform polysynthetic twinning of the mineral on (010). No less than 450 Laue photographs of the available specimen were necessary in order to find a crystal fragment which did not give diffuse reflections or double (sometimes four- or fivefold) reflections. Heating the barylite at 450-650°C reduced the stresses which continually showed up on the x-ray photographs.

With the single monocrystalline fragment, Weissenberg photographs were obtained of the 12th layer lines on rotation about the a, b, and c axes (Mo  $K\alpha$ -radiation). The unit cell parameters agreed with those given above within the limits of experimental error. The intensities of the reflections

were measured visually using a blackening chart (in steps of  $2^{1/4}$ ). Reflections with low values of  $\sin \varphi / \lambda$  (under the securing strip of the film holder) were measured from photographs taken with Cu radiation. The systematic absences corresponded to the diffraction group  $mmmPn - a$ , i. e., to two possible space groups,  $Pnma$  and  $Pn2_1a$ . A very marked piezoelectric effect, greater than that for quartz (the measurements were made by colleagues in the Crystal Physics Faculty of Moscow State University, to whom the authors are deeply indebted), was an argument in favor of the hemihedral group  $Pn2_1a$  as against the centrosymmetric group  $Pnma$ , suggested by Ygberg and Smith. Our conclusion was confirmed by a statistical analysis of the distribution of the structure factors  $F_{hk0}^2$  and  $F_{0kl}^2$ .

The presence of a Ba atom, with a scattering ability greatly exceeding that of Si, O, and Be, forced us to use in the analysis not the classical function  $N(z)$ , but a modified structure factor distribution function  $N(z, r)$  [6]. The relationship given in [6, 7],  $r = Z_T(\Sigma Z_L^2)^{-1/2}$ , in the case of barylite becomes

$$r = \frac{56}{29.56} = 1.9 \approx 2.0. \quad (1)$$

The experimental points of  ${}_1N(z, r)$  for the  $0kl$  and  $h0l$  zones fall very close to the curve for the noncentrosymmetric  $F^2$  distribution in both projections (Fig. 1).

In solving the structure we started off with 121 nonzero  $hk0$  reflections and 102 nonzero  $0kl$

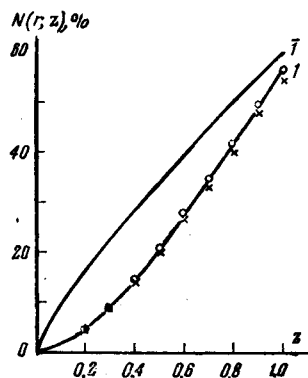


Fig. 1. Barylite. Negative result of a statistical test for a symmetry center. The two curves shown represent the centered case (1) and the noncentered case (2), together with the experimental results, where O represents the  $hk0$  zone, and x the  $0kl$  zone.

reflections. The noncentrosymmetric (but apparently close to centrosymmetric) arrangement of the atoms imposed a characteristic pattern on the Patterson projection  $p(xy)$  and  $p(yz)$ , and gave spread-out peaks from which only approximate coordinates could be found. The heavy Ba atoms considerably eased the analysis of the Patterson syntheses, and this Ba was identified on both projections. In the next step, this fixed Ba was made the basis of a modified heavy-atom approach.

It is well known that the presence of a heavy atom in centrosymmetric structures often guarantees success in structure analysis of both organic and inorganic materials. If barylite were actually centrosymmetric, then with  $r = 2.0$ , about 90% [8] of the amplitudes would have actual signs corresponding with those calculated from the Ba atom contributions. The use of the heavy-atom method for a noncentrosymmetric crystal is based on the assumption that the phase angles obtained from the heavy atom contributions are quite close to those calculated from all the atoms. In our noncentrosymmetric case, according to [9], the heavy-atom method becomes more complicated. As follows from the coordinates found roughly, in the  $xy$  projection the Ba atom lies in a position with a single free parameter. In the  $yz$  projection there is freedom to choose the origin of the coordinates but, in shifting the Ba atom to the origin, we, for purposes of calculation, artificially raise the symmetry of the distribution of the remaining atoms, making this distribution centrosymmetric. This arrangement provides the desired independent solutions for both projections.

In the  $yz$  projection we have one heavy atom with a scattering power of  $f_H$  and  $m$  light atoms with  $f_L$ . As already stated, the heavy Ba atom ( $Z = 56$ ) has been shifted to the origin of the unit cell. The phase angles of the corresponding amplitudes are obtained from the formula

$$\tan \alpha = \frac{\Sigma f_L \sin 2\pi\theta_i}{\{f_H + \Sigma f_L \cos 2\pi\theta_i\}}. \quad (2)$$

In the ideal case, where the scattering abilities of the light atom are equal,  $\Sigma f_L = m f_L$ , and Eq. (2) transforms into

$$\begin{aligned} \tan \alpha &= \frac{\sqrt{\frac{2}{m}} \Sigma \sin 2\pi\theta_i}{\{r\sqrt{2} + \sqrt{\frac{2}{m}} \Sigma \cos 2\pi\theta_i\}} \\ &= \frac{B'}{r\sqrt{2} + A'}, \end{aligned} \quad (3)$$

where  $\underline{r}$  is given in (1).

The probability of a phase angle falling in the range  $\alpha, \alpha + d\alpha$  corresponds to the probability of  $B'$  falling in the region  $y, y + dy$  and  $A'$  in the re-

gion  $x - r\sqrt{2}$ ,  $x - r\sqrt{2} + dx$ . Setting  $x = R \cos \alpha$ ,  $y = R \sin \alpha$  (4), and changing to polar coordinates, we have

$$P(\alpha) = \frac{1}{2\pi} \exp(-r^2 \sin^2 \alpha) \int_0^\infty R \exp\left\{-\frac{1}{2}(R - r \cos \alpha)^2\right\} dR$$

$$= \frac{1}{2\pi} \exp(-r^2) + \frac{r \cos \alpha}{\sqrt{\pi}}$$

$$\times \exp(-r^2 \sin^2 \alpha) \left[ \frac{1}{2} + \varphi(\sqrt{2} r \cos \alpha) \right], \quad (4)$$

where

$$\varphi(z) = \frac{1}{\sqrt{2\pi}} \int_0^z \exp(-t^2/2) dt. \quad (5)$$

Thus the fraction of the structure amplitudes  $N(\alpha)$  with a phase angle lying within the range  $-\alpha$  to  $+\alpha$  is

$$N(\alpha) = \int_{-\alpha}^{+\alpha} P(\alpha) d\alpha = 2 \int_0^{+\alpha} P(\alpha) d\alpha, \quad (6)$$

which is directly dependent on  $r$ , so that, knowing  $r$ , we will always have a clear answer to the question of the maximum phase limits of the light atoms at which we might neglect their variations from 0 to 180° (when the heavy atom is at the cell origin). When  $\alpha = 30^\circ$  its sine is already equal to  $1/2$ , and the imaginary part of the structure amplitude cannot be neglected.

Table 1 shows that for  $r = 2$  only two thirds of the phase angles fall in the range  $\pm 20^\circ$  and only about half in the range  $\pm 15^\circ$ .

We therefore have to be particularly careful about using the heavy-atom method in the  $yz$  projection; if when  $r = 2$  in a centrosymmetric crystal 98% of the structure amplitude signs are determined by the heavy-atom contribution, then for a noncentrosymmetric crystal we have 98% of the phase angles scattered through a wide range ( $\pm 53\%$ ) on both sides of the heavy-atom phase angle.

This meant that the first electron density syntheses ( $yz$ ), constructed from the heavy Ba atom,

contained a very large number of strongly smeared-out peaks. It was impossible to locate with assurance even the "medium-weight" Si atoms. The basic reason for the "dud" projection is the superposition of two structures, the true one and a "false" reflection of it in the pseudocenter of symmetry (a result of raising the symmetry by putting Ba at the origin). However, a simultaneous examination of the "complex" pattern  $\rho(yz)$  and the true one  $p(yz)$  allowed us to distinguish between the two versions of the (Ba + Si<sub>1</sub> + Si<sub>2</sub>) structure, the direct and the inverted one.

The inclusion of the two Si atoms with the Ba atom increases the effectiveness of the heavy-atom method: the parameter  $r$  increases to

$$r = \{\Sigma f_H^2 / \Sigma f_L^2\}^{1/2} = 2.7 (\approx 3.0). \quad (7)$$

Now about 70% of the phases lie between  $\pm 15^\circ$  and more than 85% lie between  $\pm 20^\circ$ , so the situation becomes very much more favorable. Of the two calculated syntheses (one for each of the combinations of Ba + Si<sub>1</sub> + Si<sub>2</sub>), one version gave no new information because of the false positioning of the atoms, and the other allowed two O atoms to be located; the coordinates of the remaining O atom were found in the subsequent syntheses.

In the  $xy$  projection, the position of Ba is fixed by a single parameter, and we have

$$P(\alpha) d\alpha = P(|F|, \alpha) d|F| d\alpha / P(|F|) d|F|, \quad (8)$$

where the numerator and denominator are the same as in [7, 10, 11]. Setting

$$x = 2|F| |F_H| / \Sigma f_L^2, \quad (9)$$

we obtain

$$P(\alpha) d\alpha = \exp(x \cos \alpha) d\alpha / 2\pi I_0(x), \quad (10)$$

where  $I_0$  is the Bessel function of the imaginary argument.

Here, as previously,

$$N(\alpha) = \int_{-\alpha}^{\alpha} P(\alpha) d\alpha. \quad (11)$$

TABLE 1

$N(\alpha)$	0	0.377	0.667	0.843	0.931	0.970	0.987	0.998	0.999
$\alpha$	0	10°	20°	30°	40°	50°	60°	90°	120°

Investigation of the relationship  $N(\alpha, x) = f(x)$  shows that as  $x$  increases, the probability that the difference  $\alpha - \alpha_H$  will be small also increases. Thus, for  $x = 1$  the probability of  $\alpha - \alpha_H$  falling in the range  $\pm 20^\circ$  will be 0.234, while for  $x = 5$  it increases to 0.549. Making the minor assumption that  $F_H \approx F$ , for the case of a single heavy atom we can conclude that

$$x \approx 2r^2. \quad (12)$$

In the  $xy$  projection the influence of the Ba atom shows up more strongly ( $x = 8$ ). The synthesis  $\rho(xy)$  constructed from the Ba atom gave quite reliable positions for both Si and one of the O atoms. The weighting function  $w(x)$  was, in accordance with [10], set equal to unity. From a subsequent series of  $\rho(xy)$  syntheses it was possible to fix the remaining O atoms. Thus, in both projections we were able to use the heavy-atom method successfully to locate all the atoms except the very light Be. The reliability factors at this stage were 13.2 and 13.7%.

To locate the Be a difference Patterson synthesis was used. The Fourier heavy-atom synthesis suffers from the deficiency that the phases of the experimental amplitudes are assigned a priori through the phases of the heavy atom and at the same time these are made the basis of the positions of the known atoms. However, for a relationship where  $Z_x/Z_H \leq 0.1$  the contributions of unknown atoms can hardly change the distribution of phases, and these atoms do not appear on the electron density maps. Conversely, in difference Patterson syntheses [12, 13], known atoms may be excluded in favor of unknown ones. If  $N$  is the total number of atoms in the unit cell,  $P$  is the fraction of known atoms, and  $Q$  is the fraction of unknown ones (so that  $N = P + Q$ ), then the structure amplitude is

$$F_N(\mathbf{H}) = \sum f_{Nj} \exp [2\pi i(\mathbf{H}, \mathbf{r}_{Nj})] = |F_N| \exp (i\alpha_N) \quad (13)$$

and

$$F_P(\mathbf{H}) = |F_P| \exp (i\alpha_P). \quad (14)$$

Here  $|F_N(\mathbf{H})|^2$  is a quantity proportional to the experimental intensities and  $F_P(\mathbf{H})$  is calculated from the coordinates of the known atoms.

Let us follow [12, 13] in examining two types of syntheses which represent "expansions" of a Patterson function, with the coefficients

$$\alpha_{\text{tot}} = |F_N|^2 |F_P| \exp i\alpha_P = |F_N(\mathbf{H})|^2 |F_P(\mathbf{H})| \times \exp \{-i2\pi(\mathbf{r}, \mathbf{H}) + i\alpha_P\} \quad (15)$$

and

$$\beta_{\text{tot}} = \frac{|F_N|^2}{|F_P|} \exp (i\alpha_P). \quad (16)$$

In this way the "expanded" Patterson syntheses lead to a structure which must stand out on a background of superfluous peaks. The background can be suppressed by a modification of the expansion coefficients (for the  $\beta$ -syntheses it is always less than for the  $\alpha$ -syntheses)\*

$$\alpha_{\text{mod}} = \left[ |F_N|^2 - |F_P|^2 - \sum f_{Q_i}^2 \right] |F_P| \exp (i\alpha_P), \quad (17)$$

$$\beta_{\text{mod}} = \left[ |F_N|^2 - |F_P|^2 - \sum f_{Q_i}^2 \right] \exp (i\alpha_P) \cdot \frac{1}{|F_P|}. \quad (18)$$

In these syntheses there are no peaks in the positions of the known atoms and they possess a very insignificant background. The successful application of the strongest  $\beta$ -syntheses is determined by the composition of the group of known atoms,  $P$ . There are two points of importance here initially, namely the necessity for the existence of a relationship between the heights of genuine and parasitic peaks which does not favor the latter, and, in addition, the number of spurious peaks present plays a part. The optimum conditions occur when  $P$  is large ( $\approx N$ ), or when only a small number of atoms are known, but these atoms are heavy with  $f_{Pj} \gg f_{Qi}$ . The  $\beta$ -syntheses are more preferable in three dimensions than on a plane, since, on projection, the parasitic peaks may add to generate maxima comparable with the maxima of the real structure. The expression  $|F_P|$  in the numerator of (18) creates a further difficulty in the  $\beta$ -syntheses: when  $|F_P| = 0$  the expansion coefficients are simply indeterminate; when  $|F_P| \neq 0$  but is nevertheless very small, the corresponding amplitudes become dominant and distort the pattern of distribution of the real atoms.

With "expansion" (18) we obtain

$$\beta_{\text{mod}} = \sum_i \sum_j f_{Q_i} \exp 2\pi i \mathbf{H}(\mathbf{r}_{Q_i} - \mathbf{r}_{Q_j}) / F_P^* + F_{Q^*} \exp (2i\alpha_P) + F_Q. \quad (19)$$

The  $\beta_{\text{mod}}$ -synthesis contains  $Q$  atoms, and does not include the  $P$  atoms, but the symmetry of the  $\beta$ -synthesis as a whole is determined by the symmetry of the distribution of these  $P$  atoms. From expression (19) it follows that the  $\beta$ -synthe-

\*We can consider syntheses with coefficients (17) and (18) as modified difference Patterson syntheses starting from  $|F_N|^2 - |F_P|^2 - \sum f_{Q_i}^2$ , using the two functions  $\exp i\alpha_P$  and  $1/|F_P|$  (or  $|F_P|$ ).

sis, in addition to the sought-after distribution  $F_0$ , contains the inverted distribution  $F_0^*$ , and also the Patterson synthesis for the unknown atoms [first term in (19)].

In view of the defects of the  $\beta$ -syntheses, basically due to the modulating functions  $1/|F_P|$  and  $\exp(i\alpha_P)$ , we prefer the difference Patterson syntheses, † which have a number of factors in their favor, i. e.:

- 1) since the vector space is necessarily centrosymmetric in the difference syntheses, only experimental intensities and moduli (squares of moduli) appear, but not phases;
- 2) there is no question of indeterminacy in series coefficients at small  $|F_P|$ ;
- 3) there is no part played in the difference Patterson syntheses by the other modulating function  $\exp(i\alpha_P)$ , which is directly connected with the position of the known atom (we do not have to carry information on the known atoms);
- 4) the general (to some degree) principle of difference syntheses, i. e., taking as the starting coefficients  $|F_{\text{exp}} - F_{\text{calc}}|$ , in

which  $F_{\text{calc}} \gg F_{\text{exp}}$ , and neglecting the remainder, is here carried out automatically.

On squaring, the large differences increase on the general background of the weak ones, but not the extreme and reverse differences with  $F_{\text{exp}} \gg F_{\text{calc}}$ , since it is these which yield the most information on the unknown atoms.

In analysis of barylite, a difference Patterson synthesis was used starting from  $(F_{\text{exp}} - F_{\text{calc}})^2$ , where  $F_{\text{calc}}$  was calculated from the two Si and seven O atoms, so that the synthesis located the Ba-Ba, Be-Be, and Ba-Be peaks. The latter showed up very clearly so that it was possible to locate the Be atoms (Fig. 2). A similar method of excluding all the concealing peaks was used successfully earlier in determination of the structure of the di(meta)fluoroberyllate  $\text{RbBe}_2\text{F}_5$  [14].

The coordinates were refined by series of successive electron-density syntheses in both of the noncentrosymmetric projections,  $xy$  and  $yz$  (Fig. 3). The final values of the reliability factors‡ were

†Of two types,  $[F_N - F_P]^2$  and  $[F_N^2 - F_P^2]$  [14].

‡Max  $\sin \theta / \lambda = 1.2 \text{ \AA}$ .  $B \approx 0.6 \text{ \AA}$ .

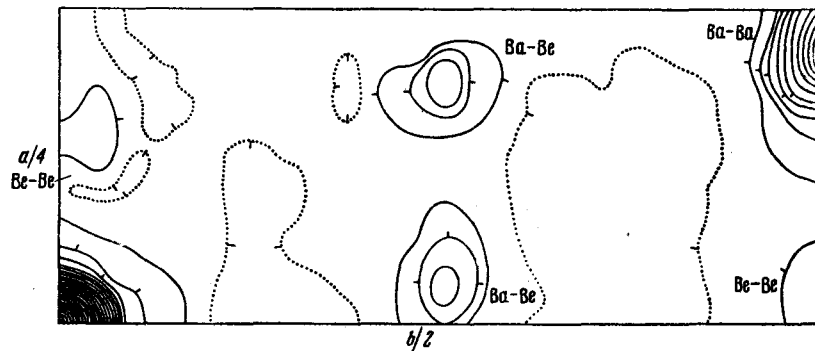


Fig. 2. The difference Patterson synthesis  $p_{\Delta}(xy)$ , with the Ba-Be and Be-Be peaks.

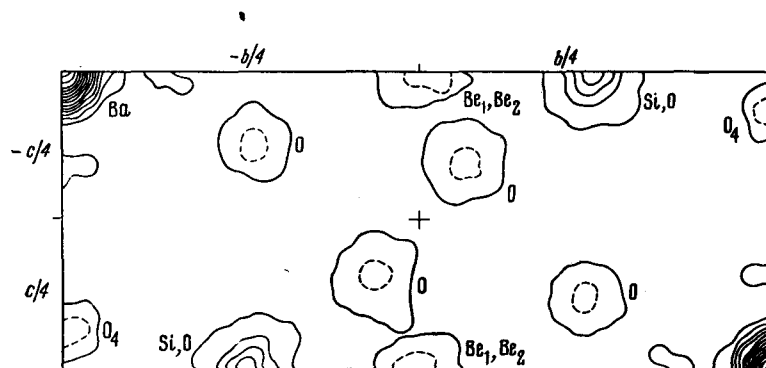


Fig. 3. Final electron density synthesis in the  $yz$  projection.

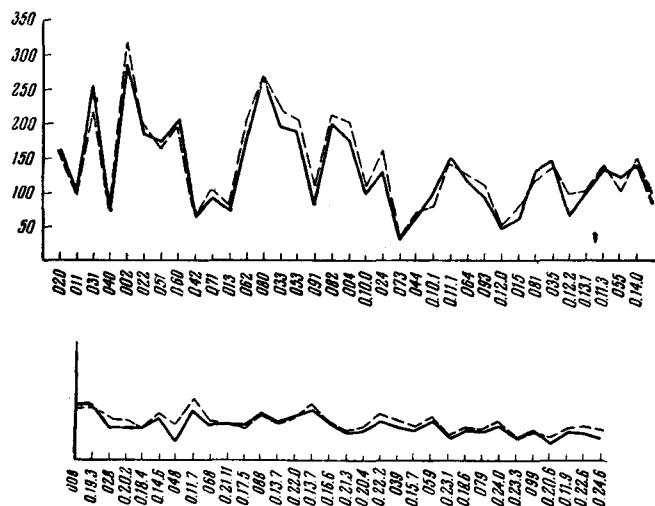


Fig. 4. Graph of convergence of  $F_{\text{exp}} - F_{\text{calc}}$  for reflections of the  $0kl$  zone.

$R_{hk0} = 11.4\%$  and  $R_{0kl} = 11.7\%$ . Figure 4 shows a graph of the convergence of  $F_{\text{exp}}$  and  $F_{\text{calc}}$  for the  $0kl$  zone. These comparatively low values of the factors are undoubtedly due to the heavy Ba atom. For greater confidence in the coordinates of the lighter atoms, the coefficients  $R'$  were calculated for the same projections, but with the Ba atom eliminated:

$$R' = \frac{\sum | |F'_{\text{exp}}| - |F'_{\text{calc}}| |}{\sum |F'_{\text{exp}}|},$$

where

$$F'_{\text{exp}} = F_{\text{exp}} - F_{\text{Ba}} \text{ \& } F'_{\text{calc}} = \sum \{F_{\text{Si}} + F_{\text{O}} + F_{\text{Be}}\}.$$

The values obtained were

$$R'_{hk0} = 18.4\% \text{ и } R'_{0kl} = 18.25\%.$$

The reliability factors  $R$  calculated for the centrosymmetric version were 28.2 and 27.6%, respec-

tively, i. e., considerably higher, in spite of the fact that the actual arrangement was not far off centrosymmetric. The coordinates of the 12 main atoms, at these values of the reliability factors, are shown in Table 2.

In a number of solved beryllium mineral structures (i. e., bromellite [16], chrysoberyl [17], bertrandite [18], euclase [19, 20]) there appears strongly expressed two-layer (hexagonal) close-packing. In berylite the single two-layer packing includes a large Ba cation in addition to the O anions. The unit cell contains  $(7 + 1) \times 4 = 32$  close-packed spheres, arranged as  $4 \times 4 \times 2$ . The greatest cell side,  $b = 11.01$  A, is determined by four O-O distances; the parameter  $a = 9.8$  A is made up of the heights of four basal triangles, and the short side  $c = 4.63$  A corresponds to the heights of two oxygen tetrahedra. How well the close-packing principle is followed can be seen from Table 2, which, together with the coordinates found experimentally, also shows those corresponding to ideal close-packing.

The berylite structure which emerges from the Fourier synthesis differs fundamentally from that noted by Ygberg in 1942. \*\* As in the majority of silicates, the basis of its construction consists of supporting columns of oxygen polyhedra around large cations, in this case of Ba. In berylite these polyhedra ("hexagonal cubo-octahedra" with coordination number 12 [22]) are packed one on the other parallel to the  $c = 4.63$  A axis. This dimension corresponds to the height of a "cubo-octahedron," but in one half of the column ( $y = b/4$ ) the Ba atoms lie at the level  $1/2$ , and in the other ( $y = 3/4b$ ) they lie at the level 0, i. e., the unit cell includes a whole polyhedron of the former and two halves of the latter (Fig. 5). Along the medium length axis, with  $a = 9.79$  A, lie two columns of each type (Fig. 6). The Ba "cubo-octahedra" present in a column

\*\*Without any proof, as pointed out in [21].

TABLE 2. Coordinates of Atoms

Atom	Ideal			Found		
	$x/a$	$y/b$	$z/c$	$x/a$	$y/b$	$z/c$
Ba	0.166	0.75	0.25	0.142	0.75	0.25
Si <sub>1</sub>	0.083	0.875	-0.125	-0.096	0.88	-0.25
Si <sub>2</sub>	-0.083	0.125	0.125	0.10	0.125	+0.25
O <sub>1</sub>	0.083	0.875	0.750	0.073	0.897	0.72
O <sub>2</sub>	-0.083	0.875	0.25	0.087	0.885	0.130
O <sub>3</sub>	0.166	0	0.25	0.181	0.03	0.452
O <sub>4</sub>	-0.166	0.75	0.75	-0.13	0.75	0.690
O <sub>5</sub>	-0.083	0.125	0.25	-0.07	0.110	0.210
O <sub>6</sub>	-0.166	0.00	0.75	-0.185	-0.025	0.595
O <sub>7</sub>	0.083	0.125	0.75	0.09	0.115	0.874
Be <sub>1</sub>	0.166	0	0.415	0.175	0.001	0.15
Be <sub>2</sub>	0.166	0	0.249	-0.170	0.005	0.25

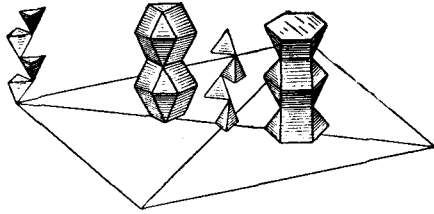


Fig. 5. The basic supporting "rods" of the barylite structure, columns of two types of Ba "cubo-octahedra" separated by polar  $[\text{Be}_2\text{O}_6]_\infty$  metachains in two orientations.

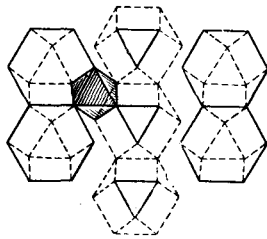


Fig. 6. The pseudocentrosymmetric distribution of Ba columns of two types. The shading picks out one of the empty octahedra, lying between the cubo-octahedra, which contains the pseudocenter of symmetry at which the origin of the unit cell lies.

of any one type are connected by shared horizontal edges. On Fig. 6 they appear to be translationally identical. The doubled parameter  $a$  (with the pseudotranslation retained) is the result of packing the spaces between the main column with parallel but polar chains of tetrahedra in which adjacent chains have opposite orientations (see the very diagrammatic Fig. 5). From their formula  $[\text{Be}_2\text{O}_6]_\infty$ , they are analogous to the metasilicate pyroxene chains  $[\text{Si}_2\text{O}_6]_\infty$ , but the axes of the latter lie in the planes of close-packing, while in the metaberyllate chain its axis ( $2_1$ ) is perpendicular to this plane. The repeat distance of such a chain (two tetrahedra) corresponds to the repeat distance of the two-layer (i. e., normal hexagonal) packing which forms the basis of the barylite structure, similar to the situation in the series of Be minerals noted above, especially the Be silicates.

The same feature [23] is also characteristic, usually with a repetition of the Be-motif, in Zn minerals, e. g., clinohedrite [24], hodgkinsonite [25], hopeite [26], and zincite ZnO. Moreover, in

all these minerals, whenever there is an appreciable content of Be (Zn) the tetrahedra around these elements line up into the metaberyllate (metazincate)  $[\text{Be}_2\text{O}_6]_\infty - [\text{Zn}_2\text{O}_6]_\infty$  chains described above. As mentioned above, these chains are polar but the majority of the structures listed contain the two sorts of chain with opposite polarities. This occurs also in barylite, i. e., its structure is extremely close to being centrosymmetric, but it does not quite "make it," as in beryllonite, bertrandite, and in barylite. With this marked hexagonal motif, deviation from the maximum symmetry is explained in [23] by the low atomic number of Be, which does allow its (ionic or atomic) framework to take on strictly spherical symmetry.

Metaberyllate (metazincate) chains have another characteristic feature; they are "encrusted" with a layer of discrete  $\text{SiO}_4$  orthotetrahedra (sometimes  $\text{PO}_4$  tetrahedra), as shown in Fig. 7. These encrusted chains are individual in euclase (clinohedrite, hopeite, hodgkinsonite), but in bertrandite and barylite the encrusting Si tetrahedra are joined through a (pseudo) plane of symmetry into diorthogroups,  $\text{Si}_2\text{O}_7$ , with axes normal to the metachain axes. †† The  $\text{Si}_2\text{O}_7$  diorthogroups join up metachains of like polarity, i. e., barylite has two types of diorthogroups, with unlike polarities. In bertrandite the metachains are all of the same polarity and have a shared O atom, while in barylite the metachains of the two orientations remain individual.

†† Ygberg [3] suggested that the structure contained diorthogroups with axes along the long axis,  $b = 11.65 \text{ \AA}$ .

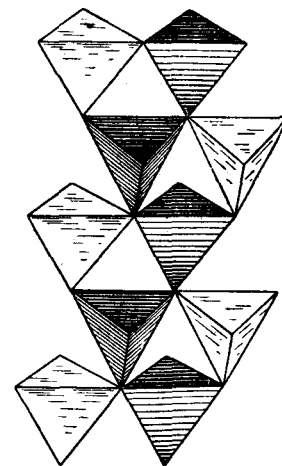


Fig. 7. Polar  $[\text{Be}_2\text{O}_6]_\infty$  metachains, encrusted with  $\text{SiO}_4$  orthotetrahedra.

TABLE 3. Interatomic Distances in the Structure of Barylite (in Å)

Si <sub>1</sub> -tetrahedron		Be <sub>1</sub> -tetrahedron	
Si <sub>1</sub> -O <sub>1</sub> = 1.63	O <sub>1</sub> -O <sub>2</sub> = 2.71	Be <sub>1</sub> -O <sub>3</sub> = 1.64	O <sub>1</sub> -O <sub>8</sub> = 2.59
Si <sub>1</sub> -O <sub>2</sub> = 1.65	O <sub>1</sub> -O <sub>4</sub> = 2.70	Be-O <sub>1</sub> = 1.65	O <sub>1</sub> -O <sub>7</sub> = 2.66
Si <sub>1</sub> -O <sub>4</sub> = 1.67	O <sub>1</sub> -O <sub>6</sub> = 2.78	Be-O <sub>7</sub> = 1.68	O <sub>1</sub> -O <sub>6</sub> = 2.69
Si <sub>1</sub> -O <sub>6</sub> = 1.64	O <sub>2</sub> -O <sub>4</sub> = 2.64	Be-O <sub>6</sub> = 1.70	O <sub>3</sub> -O <sub>7</sub> = 2.70
	O <sub>2</sub> -O <sub>6</sub> = 2.69		O <sub>3</sub> -O <sub>8</sub> = 2.64
	O <sub>4</sub> -O <sub>6</sub> = 2.75		O <sub>6</sub> -O <sub>7</sub> = 2.63
Si <sub>2</sub> -tetrahedron		Be <sub>2</sub> -tetrahedron	
Si <sub>2</sub> -O <sub>3</sub> = 1.68	O <sub>3</sub> -O <sub>4</sub> = 2.68	Be <sub>2</sub> -O <sub>2</sub> = 1.65	O <sub>3</sub> -O <sub>5</sub> = 2.70
Si <sub>2</sub> -O <sub>4</sub> = 1.70	O <sub>3</sub> -O <sub>5</sub> = 2.76	Be-O <sub>5</sub> = 1.68	O <sub>2</sub> -O <sub>3</sub> = 2.66
Si <sub>2</sub> -O <sub>5</sub> = 1.65	O <sub>3</sub> -O <sub>7</sub> = 2.67	Be-O <sub>3</sub> = 1.69	O <sub>2</sub> -O <sub>6</sub> = 2.67
Si <sub>2</sub> -O <sub>7</sub> = 1.64	O <sub>4</sub> -O <sub>5</sub> = 2.74	Be-O <sub>6</sub> = 1.66	O <sub>3</sub> -O <sub>5</sub> = 2.60
	O <sub>4</sub> -O <sub>7</sub> = 2.63		O <sub>3</sub> -O <sub>6</sub> = 2.64
	O <sub>5</sub> -O <sub>7</sub> = 2.76		O <sub>6</sub> -O <sub>7</sub> = 2.68
Ba-polyhedron			
Ba-O <sub>1</sub> = 2.82	Ba-O <sub>3</sub> = 3.34		
Ba-O <sub>5</sub> = 2.84	Ba-O <sub>6</sub> = 3.00		
Ba-O <sub>4</sub> = 3.04	Ba-O <sub>2</sub> = 2.93		
Ba-O <sub>4</sub> = 2.86	Ba-O <sub>3</sub> = 3.06		
Ba-O <sub>8</sub> = 3.12	Ba-O <sub>7</sub> = 2.89		
Ba-O <sub>6</sub> = 3.10	Ba-O <sub>7</sub> = 3.08		

The metaberyllate chains and the Si<sub>2</sub>O<sub>7</sub> diorthogroups (in the other two directions) together form a three-dimensional framework ("braid") of tetrahedra, similar to the framework in normal aluminosilicates. In the barylite framework there are also wide hollows occupied by the massive Ba cations. Their arrangement on two levels is reminiscent of that in sodalite [22], where, however, the hollows are of greater volume; they contain, in addition to the central Cl atom, another  $8 \times \frac{1}{2} = 4$  Na atoms (in the eight windows). The barylite hollows each possess only four windows. A fundamental difference between the beryllsilicate and aluminosilicate frameworks is in the number of tetrahedra in contact at a shared O corner. In aluminosilicates this is always two tetrahedra, while in beryllsilicate two tetrahedra converge on an O atom only in the centers of the Si<sub>2</sub>O<sub>7</sub> groups. Of the other six O atoms, four are shared between 1 Si + 2 Be, and two between 1 Si + 1 Be. The valence deficiency is covered by the presence of the Ba ( $2 \times \frac{1}{2}$ ). This is the reason for a certain excess charge on the other two types of O. The large size of the Ba cation, with 12 neighbors at various distances (see Table 3), does not allow it to settle the balance of valences with an accuracy greater than 0.33 units of charge. The barylite framework, of two types of tetrahedra with hollows occupied by large spherical Ba cations, is depicted in Fig. 8. Attention is drawn to the fact that the origin of the unit cell (the pseudocenter of symmetry) "hangs in space." This is not quite true; it lies in the center of an empty octahedron (picked out by shading in Fig. 6) to which are attached two metachains of different polarities, and also two diorthogroups, also of different orientation.

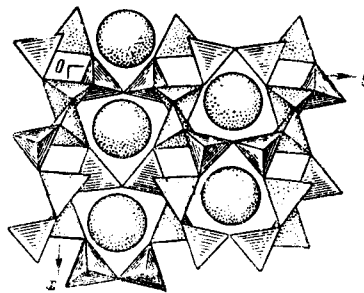


Fig. 8. General view of the barylite structure (xy projection) with a three-dimensional beryllium-oxygen-silicon framework of tetrahedra (paired Si tetrahedra are shown striated). In the large hollows lie the Ba cations.

In Table 3 are given the interatomic distances in barylite: Si-O does not lie outside the limits 1.63-1.70 Å, where, as usual, the greatest Si-O distance is that to the central atom in the Si<sub>2</sub>O<sub>7</sub> group. The length of the O-O edge varies from 2.63 to 2.78 Å. An essential feature of the diorthogroup is the angle Si-O-Si = 141°. In the metachains Be-O = 1.64-1.70 Å, with edges of length O-O = 2.59-2.70 Å. The closest 12 Ba-O distances lie in the range 2.82-3.34 Å.

The columns of Ba cations and the parallel chain of Be tetrahedra make barylite optically positive. The (010) cleavage is parallel to the plane in which the axes of the Si<sub>2</sub>O<sub>7</sub> diorthogroups lie, and parallel to it are the [Be<sub>2</sub>O<sub>6</sub>]<sub>∞</sub> chains. The other cleavage, (210), corresponds to the diagonal of a cell with a value of a half the normal, i.e., that at which columns with an identical height of Ba atoms would be translationally identical. It is easy to see that this cleavage also does not intersect the Si<sub>2</sub>O<sub>7</sub> groups and is parallel to the [Be<sub>2</sub>O<sub>6</sub>]<sub>∞</sub> chains.

It has been pointed out that barylite, like a number of other Be minerals including the very simple bromellite BeO, has a characteristic single two-layer close-packing, but in barylite the large Ba cation participates on equal terms (in the ratio 1:7) in this packing. In the light of this, a discovery made by one of the present authors [23] must seem natural: that chemically pure "Kalbaum" BeO contained up to 0.2% BaO, while natural BeO, bromellite, contained up to 1.5% BaO. This paradox becomes easily understood if we assume that the very feasible introduction occurs (on the "soil" of the single close-packing layer) of very fine inclusion of barylite into BeO (as intergrowth or attachment).

## LITERATURE CITED

1. A. G. Zhabin and M. E. Kazakova, DAN SSSR, 134, No. 2 (1960).
2. G. Aminoff, Geol. fören. i Stockholm. förhandl., 45, 197 (1923).
3. E. R. Ygberg, Geol. fören. i Stockholm. förhandl., 134, 394 (1941).
4. J. C. Smith, Amer. Mineralogist, 41, 512 (1956).
5. H. Strunz, Mineralogical Tables [Russian translation] (IL, Moscow, 1962).
6. G. A. Sim, Acta crystallogr., 11, 123 (1958).
7. W. Cochran, Acta crystallogr., 8, 473 (1955).
8. G. A. Sim, Acta crystallogr., 10, 177 (1957).
9. G. A. Sim, Acta crystallogr., 10, 536 (1957).
10. G. A. Sim, Acta crystallogr., 12, 813 (1959).
11. V. V. Ilyukhin, Kristallografiya, 7, 5, 680 (1962) [Soviet Physics - Crystallography, Vol. 7, p. 551].
12. G. N. Ramachandran and S. Raman, Acta crystallogr., 12, 957 (1959).
13. S. Raman, Acta crystallogr., 14, 148 (1961).
14. V. V. Ilyukhin and N. V. Belov, Kristallografiya 6, 6, 847 (1961) [Soviet Physics - Crystallography, Vol. 6, p. 685].
15. N. V. Belov, Crystal Chemistry of Large-Cation Silicates [in Russian] (Izd. AN SSSR, 1961).
16. Strukturbericht, 1, No. 78, 115.
17. W. L. Bragg and G. B. Brown, Z. Kristallogr., 63, 122 (1926).
18. L. P. Solov'eva and N. V. Belov, DAN SSSR, 140, 3, 685 (1961).
19. J. Biscoe and B. E. Warren, Z. Kristallogr., 86, 292 (1933).
20. V. V. Bakakin and I. Kh. Al'tshuller, Zh. struktur. khimii, 2, 66 (1961).
21. Strukturbericht, 9, 253 (1955).
22. K. K. Abrashev and N. V. Belov, DAN SSSR, 144, 3, 636 (1962).
23. N. V. Belov, Mineralog. sb. L'vovsk geol. obsh. pri univ., 16 (1962).
24. A. V. Nikitin and N. V. Belov, DAN SSSR, 148, No. 6 (1963).
25. L. P. Solov'eva and N. V. Belov, DAN SSSR, 152, 2, 327 (1963) [Soviet Physics - Doklady, Vol. 8, p. 867].
26. R. S. Gamidov, V. P. Golovachev, Kh. S. Mamedov, and N. V. Belov, DAN SSSR, 150, No. 2 (1963).

---

All abbreviations of periodicals in the above bibliography are letter-by-letter transliterations of the abbreviations as given in the original Russian journal. *Some or all of this periodical literature may well be available in English translation.* A complete list of the cover-to-cover English translations appears at the back of this issue.